Sensitivity Analysis in Energy Hubs of Official Buildings Considering Renewable Energy Resources and CHP

Sajad Sadi[1], Masoud Alilou[2,*]

[1] *Department of mechanical engineering, Imam Hossein Comprehensive University, Tehran, Iran*
[2] *Department of Electrical Engineering, Engineering Faculty of Khoy, Urmia University of Technology, Urmia, Iran*
**Corresponding author: masoud.alilou@gmail.com*

Manuscript received 17 July, 2025; revised 14 November, 2025; accepted 19 November, 2025. Paper no. JEMT-2507-1565.

Energy hubs provide a unified platform for managing electricity, gas, and thermal energy; however, their responsiveness to uncertain operational conditions remains insufficiently addressed. To fill this gap, a single-building energy hub is modeled using real-world data from diverse Iranian climates in this paper. This study models a single-building energy hub using real-world data from diverse Iranian climates and introduces a sensitivity-driven optimization framework for official buildings. The configuration includes grid electricity, wind turbines, photovoltaic panels, geothermal pumps, solar water heaters, diesel generators, and natural gas. A mixed-integer programming approach minimizes operating costs under technical and policy constraints. Sensitivity analysis reveals that integrating renewable energy sources reduces operational costs by up to 27%, while CHP deployment alone achieves a 19% cost reduction under gas price volatility. Grid outages increase costs by 35% and lead to up to 22% load curtailment. These findings offer a scalable framework for designing resilient energy systems tailored to administrative infrastructure under uncertainty.

Keywords: *Sensitivity analysis; Energy hub; Official buildings; Renewable energy; Combined heat and power*

http://dx.doi.org/10.22109/jemt.2025.535292.1565

Nomenclature

T_P	Time horizon
N_T	Number of time periods
LT	Equipment life-time
d	Interest rate
$Cost^t_{P-grid}$	Cost of exchanging electrical energy with the grid
$Cost^t_{g-grid}$	Cost of supplying heat directly from the national gas network in the engine room
$Cost^t_{P-CHP}$	Cost of producing a CHP unit
$Cost^t_{P-RE}$	Cost of operating of renewable units
$Cost^t_{P-batt}$	Cost of fully charging the battery
ρ^t_{buy}	Purchase price of electricity from the national grid at time t
ρ^t_{sell}	Cost of selling electricity per kWh upstream at time t
S^t_{buy}	Amount of power exchanged from the network to the microgrid at time t
S^t_{sell}	Amount of power exchanged from the microgrid to the network at time t
AC_M	Annual investment cost of the building engine room
S^t_M	Optimal heat capacity of the engine room
C^t_M	Cost of O&M thermal engine room
q^t_M	Volume of gas consumed by the engine room
ρ^t_{gas}	Rate per cubic meter of natural gas
r_M	Gas consumption rate by engine room
AC_{CHP}	Annual investment cost of CHP
S^t_{P-CHP}	Optimal electrical capacity of CHP
S^t_{H-CHP}	Optimal thermal capacity of CHP
C^t_{P-CHP}	Cost of the O&M electrical section of CHP
C_{H-CHP}	Cost of the O&M thermal section of CHP
q^t_{CHP}	Volume of gas consumed by CHP
ρ^t_{gas}	Rate per cubic meter of natural gas
r_{CHP}	Gas consumption rate by CHP
AC_x	Investment cost of each equipment
C_x	O&M cost of each equipment
r_{GT}	Rate of electricity consumption of the geothermal unit
r_{solar}	Rate of electricity consumption of the solar water heater unit
AC_{batt}	Investment cost of ESS

S_{batt}^{t}	Optimal capacity of ESS
C_{batt}	O&M cost of ESS at time t
η_{x_e}	Electrical efficiency of the unit
η_{x_H}	Thermal efficiency of the unit
P_{P-L}^{t}	Annual peak of electric load of the network
H_{P-L}^{t}	Annual peak of thermal load of the network
$S_{wind\_max}^{t}$	Maximum power wind turbine
E	Amount of energy received from the sun
P_{DR}^{t}	Electric peak load of demand response
H_{DR}^{t}	Thermal peak load of demand response
CHP	Combined heat and power
PV	Photovoltaic panel
WT	Wind turbine
EV	Electric vehicle
GT	Geothermal source
SWH	Solar water heater
ESS	Energy storage source
CC	Capital cost
OC	Operation cost
O&MC	Operation and maintenance
FC	Fuel cost
AC	Annual cost

1. Introduction

Energy hub has emerged as a novel concept in power systems. It offers a multi-carrier framework that enables the integration, conversion, and management of diverse energy forms [1]. Energy hubs provide a flexible platform for optimized energy flow and system-level coordination by facilitating the interaction between electricity, gas, thermal energy, and other carriers [2]. Their scalable nature allows implementation across various levels, from individual buildings to city-wide infrastructures, making them a pivotal tool in modern energy planning [3].

At the core of an energy hub lies the capacity to transform, store, and distribute energy through an interconnected network of components including transformers, combined heat and power (CHP) units, power electronic devices, compressors, heat exchangers, and energy storage systems [4]. These elements collectively support multi-energy management, enhance system reliability, and improve operational flexibility. On the other hand, the integration of renewable energy resources such as photovoltaic (PV) systems and wind turbines (WT) within energy hubs has further elevated their role in promoting sustainability and reducing dependence on fossil fuels [5]. Coupled with CHP technologies, which efficiently generate electricity and usable thermal energy from a single source, energy hubs are positioned to maximize energy efficiency and enable resilient operation under variable supply conditions [6]. From a systems perspective, the coordinated use of multiple energy carriers offers several advantages, including the enhanced reliability through diversified energy sources, the increased load adaptability and operational agility, synergistic effects that improve overall system performance, and substantial potential for cost and emissions optimization [7-8]. These multifaceted benefits underscore the growing importance of energy hubs as a strategic solution for meeting evolving energy demands in official and administrative buildings [9].

Energy optimization has been extensively studied across various domains [10–11], with a notable focus on the operational planning of CHP systems. A mathematical model for CHP systems aiming to minimize costs in small-scale applications was proposed in [12], while [13] introduced a linear programming approach considering operational constraints. Studies such as [14] explored CHP integration alongside separate thermal generation in restructured markets, and [15] examined the synergy between CHP and energy storage systems. More recently, the coordinated operation of multi-energy systems has gained attention. For instance, [16] developed a framework for simultaneous use of CHP, PVs, and electrical storage. Distributed generation and electric vehicle interactions were investigated in [17], while [18–19] analyzed joint operation of PV panels, CHP units, and gas turbines. Energy management in such multi-carrier systems is further examined in [20]. A modeling framework for load flow studies in energy hubs using matrix-based input-output relationships was introduced in [21], employing multi-agent genetic algorithms for decentralized optimization. Challenges posed by the variability of renewable resources within energy hubs are discussed in [22], particularly with respect to probabilistic economic dispatch in the presence of wind energy. Efforts to optimize energy cost under uncertainty include robust management strategies such as those in [23], implemented in Waterloo, Canada using dynamic integer programming. Economic valuation of inputs and outputs along with CHP and energy storage integration, are examined in [24]. This study adopts Monte Carlo simulation for long-term price modeling but omits renewable sources. Short-term energy hub operation under uncertainties like wind variability, market prices, and load dynamics is addressed in [25]. This model features diverse inputs (electricity, gas, water, wind), outputs (electricity and heat), and internal components such as CHP, boilers, and energy storage. The wind profile is treated deterministically using forecasted values. Electric vehicle modeling within renewable-based energy hubs is proposed in [26], detailing a two-stage optimization process that considers charging costs and network impact. Reference [27] explores multi-objective optimization for inter-area power flow, focusing on economic and reliable system performance, though without modeling internal hub dynamics. Advanced formulations for energy hub design, including mixed-integer linear programming to handle conversion efficiencies and storage losses, are discussed in [28]. Inputs include electricity, natural gas, and solar panels. Residential-scale studies are also abundant: [29] and [30] address smart homes with CHP and EVs, targeting consumer cost minimization through demand awareness and energy price response. Reference [31] incorporates demand-side management and multi-objective optimization to reduce greenhouse gas emissions. Dynamic thermal demand modeling using Markov Chain Monte Carlo simulation is introduced in [32], emphasizing cross-carrier energy interactions. Small-scale storage impacts are evaluated in [33] with control strategies that enhance cost performance. Ref. [34] presents a mixed-integer framework for locating and controlling household energy systems. It effectively models a specialized case of residential energy hubs.

In another research, Zhou et al. [35] proposed a stochastic distributional robust optimization framework for integrated electricity and heat systems, focusing on network hardening and storage deployment under extreme event uncertainty. Similarly, Han et al. [36] developed a stochastic gradient-enhanced optimization model for multi-energy systems, incorporating probabilistic resource availability and outage scenarios. While these models emphasize resilience, they are primarily designed for large-scale urban networks and lack the granularity needed for building-level energy hubs. In contrast, this study introduces a sensitivity-driven optimization framework tailored to official buildings, using real-world climatic and load data to evaluate system responsiveness under variable conditions. The table 1 summarizes key differences between existing models and our proposed approach.

Table 1 Comparison of models of [35] and [36] with proposed framework

Item	Reference		
	[35]	[36]	This study
Optimization type	Stochastic robust optimization	Resilience-oriented MILP	MILP with scenario-based sensitivity
Uncertainty handling	Renewable & load uncertainty	Outage scenarios & adaptive dispatch	Parametric input variation
System scale	Urban networks	City-wide hubs	Single-building hubs
Application domain	Electricity & heat systems	Multi-energy systems	Official buildings
Renewable integration	Moderate	Partial	Extensive
Sensitivity analysis	No	No	Yes

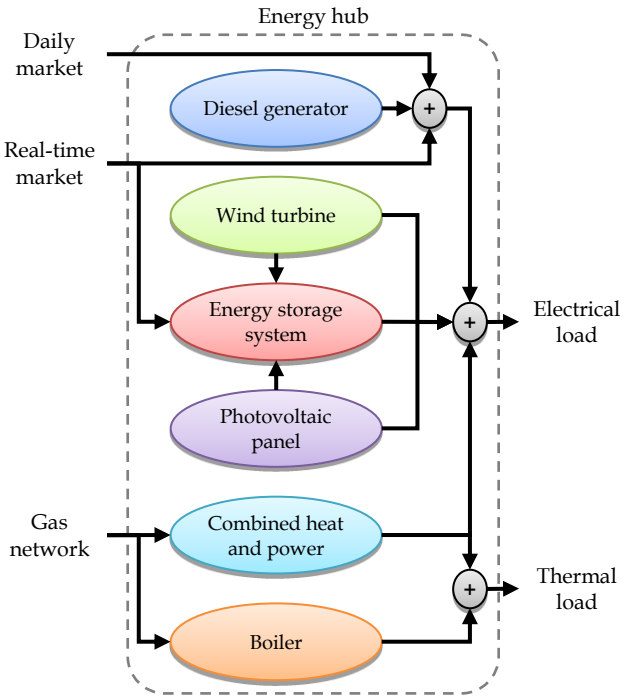

Fig. 1 Electrical and thermal energy components in the studied energy hub

Despite extensive research on multi-energy systems and energy hub optimization, several critical gaps persist. Most existing studies focus on deterministic models or isolated energy carriers, overlooking the dynamic and uncertain nature of real-world operations. In particular, the responsiveness of energy hubs to fluctuations in resource availability, market prices, and grid reliability remains underexplored. This issue is especially pronounced in official buildings, where energy continuity is vital and policy constraints often limit flexibility. Moreover, few studies offer sensitivity-driven frameworks that evaluate how input-output dynamics shift under diverse climatic and infrastructural conditions. Addressing these gaps is essential for designing resilient, cost-effective energy systems tailored to administrative environments. So, this study proposes a novel modeling and optimization framework for a single-building energy hub tailored to official buildings. The main contributions of the paper are as follows:

- Development of a unified energy hub model designed to the thermal and electrical demands of administrative buildings in various Iranian climates.
- Integration of renewable energy carriers, including wind turbines, photovoltaic panels, geothermal heat pumps, and solar water heaters, alongside conventional sources such as grid electricity, natural gas, and diesel generators.
- Formulation of a cost-minimization optimization problem with decision variables representing energy carrier shares, subject to technical, capacity, and policy constraints.
- Implementation of scenario-based sensitivity analysis to assess how changes in input availability and pricing affect operational cost, system performance, and energy supply continuity.
- Application of real-world data, including regional load profiles, price trends, and renewable potential, to validate the model and reflect geographically relevant energy behavior.

So, in this study, the energy hub for each building is modeled as a standalone unit with defined input carriers and output loads. The proposed framework employs dynamic scheduling to determine the optimal distribution of energy resources over time. After identifying the system's optimal operating points, the paper applies parametric sensitivity tests, such as reduced availability of wind power, natural gas cuts, or loss of grid electricity, to measure shifts in operational strategy and cost impact. Sensitivity analysis is employed to investigate how variations in input quantities, prices, and resource availability affect operational cost, system reliability, and energy distribution.

The remainder of the paper is organized as follows. Section 2 defines the problem statement and formulates the mathematical model, including the objective function and operational constraints related to energy balancing, equipment capacities, renewable integration, ground space, and demand-side policies. Section 3 outlines the optimization algorithm used to minimize operating costs while ensuring system feasibility. Section 4 presents the results of sensitivity analyses, evaluating how variations in energy availability, market prices, and technical limitations impact system performance and reliability. Section 5 concludes the study with key findings, practical implications, and recommendations for future research.

2. Problem Statement and Formulations

Determining the optimal capacity of different equipment in an energy hub is done in this section by considering the system constraints and with the aim of minimizing the cost of energy supply. Due to the high number of buildings, by optimizing consumption according to the proposed solution, significant savings in energy consumption and supply costs are made. On the other hand, due to the influence of renewable energy-based distributed generation, optimal capacity planning faces new complexities and challenges. The main reason for this complexity is the dependence of the output power of these products on climatic conditions. This section describes the various components of the proposed energy management system.

The proposed model consists of two main parts. The first part is the objective functions related to the optimal planning of the energy hub equipment. In this section, the optimal installed capacity to supply electrical and thermal load of the energy hub is determined. The second part of the optimal operation constraints is defined as two categories of functional constraints and policy-making. At the end of this section, an hour-by-hour model for energy management and control of installed equipment, in addition to the defined project, is performed. It should be noted that the optimal operation is on an hourly basis and only for very large centers and large towns with a dispatching center. Candidate equipment for the supply of electrical and thermal energy for the energy hub is shown in Figure 1.

In this section, a planning model for the investment horizon and in specific time periods is proposed. This model determines the optimal capacity for energy hub equipment including engine room and CHP

units, renewable units such as WTs, PVs, geothermal (GT) sources and solar water heaters (SWHs) and energy storage source (ESS). In other words, the output of this model shows that in order to provide the optimal annual thermal and electrical peak load on the planning horizon, the energy hub must be equipped with what equipment and with what capacities [37-38].

The proposed scheduling problem is specified in the T_P time horizon and for the number of N_T time periods. This means that the purpose of planning is to equip the energy hub for an annual T_P time horizon. This horizon is divided into N_T periods when each period is T_P/N_Tyears. Planning is done for the first course. Subsequent periods determine the amount of capacity upgrade of equipment. For better understanding in the form of an example, if the total time horizon studied is assumed to be 10 years, this horizon is divided into two periods of 5 years. The optimal capacity obtained for each unit in the second 5 years minus the optimal capacity of the same unit in the first 5 years determines the rate of capacity upgrade. The objective function is obtained from the total cost of all the units that make up the energy hub. The cost function of CHP unit and units based on renewable energy includes two parts: capital cost (CC) and operation cost (OC). The CC includes two costs, namely the operation and maintenance (O&MC) and the fuel cost (FC). The CC includes the purchase of equipment charge, their installation and the cost of obtaining the necessary permits. It should be noted that the equivalent annual cost (AC) for each of the equipment is calculated as by Eq. (1):

$$AC = \frac{d(1+d)^{LT}}{(1+d)^{LT}-1} * CC \tag{1}$$

This equation determines the annual investment cost for equipment based on the total equipment investment cost, equipment life-time (LT) and interest rate (d). Using this relationship, the investment cost of equipment is divided over their lifetime, and for each year of operation, the annual investment cost will be added to the objective function. In this way, the effect of the life of equipment will be considered in its selection for optimal energy hub planning. In this paper, according to the topics of engineering economics, in order to convert future costs (time period t) to current costs, the coefficient β(t) has been used. This coefficient is obtained using Eq. (2).

$$\beta(t) = \frac{1}{(1+d)^t} \tag{2}$$

Here, d shows the interest rate.

2.1. Objective function

The cost of planning depends on the unit capacity. It should be noted that the fuel cost of renewable units is zero. Therefore, the mathematical expression of the objective function for planning time periods is as equation (3).

$$F_P = \sum_{T_P} \left(Cost^t_{P-grid} + Cost^t_{g-grid} + Cost^t_{P-CHP} + Cost^t_{P-RE} + Cost^t_{P-batt}\right) \tag{3}$$

Where, $Cost^t_{P-grid}$, $Cost^t_{g-grid}$, $Cost^t_{P-CHP}$, $Cost^t_{P-RE}$, and $Cost^t_{P-batt}$ represent the cost of exchanging electrical energy with the grid, the cost of supplying heat directly from the national gas network in the engine room, the cost of producing a CHP unit, the cost of operating of renewable units, and the cost of fully charging the battery, respectively.

The cost of exchanging electrical energy with the grid is calculated by Eq. (4).

$$Cost^t_{P-grid} = \sum_T [(\rho^t_{buy}.S^t_{buy}) - (\rho^t_{sell}.S^t_{sell})] * \beta(t) \tag{4}$$

According to Equation (4), ρ^t_{buy} is the purchase price of electricity from the national grid and ρ^t_{sell} is the cost of selling electricity per kWh upstream. In this regard, S^t_{buy} is the amount of power exchanged from the network to the microgrid and S^t_{sell} is the amount of power exchanged from the microgrid to the network in time period t. According to the above relation, this cost depends on the price of buying or selling electricity to the electricity network and the amount of exchange power with the network.

The cost of supplying heat directly from the national gas network in the engine room is calculated by Eq. (5).

$$Cost^t_{g-grid} = \sum_T AC_M * \beta(t) * (S^t_M) + C^t_M S^t_M * \beta(t) + \rho^t_{gas}.q^t_M \tag{5}$$

Here, AC_M is the annual investment cost of the building engine room, and S^t_M is the optimal heat capacity of the engine room. C^t_M is the cost of O&M thermal engine room. q^t_M is the volume of gas consumed by the engine room and ρ^t_{gas} is the rate per cubic meter of natural gas. This equation presents that the cost of fuel in the above cost function is proportional to the volume of gas consumed. The volume of gas consumed depends on the gas consumption rate (r_M). It is presented using Eq. (6).

$$q^t_M = (S^t_M) * r_M \tag{6}$$

Equation (7) is utilized to calculate the cost of producing a CHP unit.

$$Cost^t_{P-CHP} = \sum_T AC_{CHP} * \beta(t) * (S^t_{P-CHP} + S^t_{H-CHP}) + C^t_{P-CHP} * S^t_{P-CHP} + C_{H-CHP}.S^t_{H-CHP} * \beta(t) + \rho^t_{gas}.q^t_{CHP} \tag{7}$$

Where, AC_{CHP} is the annual investment cost of CHP, S^t_{P-CHP} and S^t_{H-CHP} is the optimal electrical and thermal capacity of CHP. C^t_{P-CHP} and C_{H-CHP} are the cost of the O&M electrical and thermal section of the CHP. q^t_{CHP} is the volume of gas consumed by CHP and ρ^t_{gas} is the rate per cubic meter of natural gas. According to the above relation, the fuel cost in the CHP cost function is proportional to the volume of gas consumed. The volume of gas consumed depends on the gas consumption rate (r_{CHP}). This relationship is presented in Eq. (8).

$$q^t_{CHP} = (S^t_{P-CHP} + S^t_{H-CHP}) * r_{CHP} \tag{8}$$

The cost of operating of renewable units is calculated by Eq. (9).

$$Cost^t_{P-RE} = \sum_T Cost^t_{PV} + Cost^t_{Wind} + Cost^t_{Solar} + Cost^t_{GT} \tag{9}$$

$$Cost^t_{PV} = \sum_T AC_{PV} * S^t_{PV} * \beta(t) + C_{PV} * S^t_{PV} * \beta(t) \tag{10}$$

$$Cost^t_{Wind} = \sum_T AC_{wind} * S^t_{wind} * \beta(t) + C_{wind} * S^t_{wind} * \beta(t) \tag{11}$$

$$Cost^t_{Solar} = \sum_T AC_{solar} * S^t_{solar} * \beta(t) + C_{solar} * S^t_{solar} * \beta(t) + S^t_{solar} * r_{solar} * \rho^t_{buy} \tag{12}$$

$$Cost_{GT}^{t} = \sum_{T} AC_{GT} * S_{GT}^{t} * \beta(t) + C_{GT} * S_{GT}^{t} * \beta(t) + S_{GT}^{t} * r_{GT} * \rho_{buy}^{t} \quad (13)$$

In the above relations, AC_x is the investment cost and C_x is the O&M cost of each equipment. x is also the optimal capacity determined for each of the renewable resources in the planning period t. Since the geothermal unit and the solar water heater unit usually have a pump to change the water pressure (or internal fluid), electricity is used in these two renewable units to supply heat; Therefore, the amount of their consumed electricity is considered. r_{GT} and r_{solar} are the rates of electricity consumption of the geothermal unit and the solar water heater unit. Among the two common types of lead-acid and lithium-ion batteries, lead-acid batteries are not economical due to the need for high maintenance and lithium-ion batteries have been used. At the same time, its energy density is also very suitable. Because the Li-Ion battery is used, the O&M cost is zero.

Equation (14) is used to calculate the cost of fully charging the battery.

$$Cost_{batt}^{t} = \sum_{T} AC_{batt} * S_{batt}^{t} * \beta(t) + C_{batt} * S_{batt}^{t} * \beta(t) + \rho_{buy}^{t} * S_{batt}^{t} \quad (14)$$

Here, AC_{batt} is the investment cost and S_{batt}^{t} is the optimal capacity and C_{batt} is the O&M cost set for the source of electrical energy storage in the planning period t.

2.2. Constraints and limitations

The constraints of the studied model are divided into two categories: functional constraints and policy constraints. The mathematical model of these constraints is as follows [39-41]:

1) Power balance constraint: The production and consumption capacity of the energy hub must be equal per hour. For this reason, constraints (15) and (16) are considered.

$$S_{buy}^{t} + (S_{batt}^{t} * \eta_{batt}) + (S_{P-CHP}^{t} * \eta_{CHP_e}) + (S_{wind}^{t} * \eta_{solar} + S_{PV}^{t} = P_{P-L}^{t} \quad (15)$$

$$(S_{M}^{t} * \eta_{M}) + (S_{H-CHP}^{t} * \eta_{CHP_H}) + (S_{GT}^{t} * \eta_{GT}) + (S_{solar}^{t} * \eta_{solar}) = H_{P-L}^{t} \quad (16)$$

In these equations, η_{x_e} and η_{x_H} are the electrical and thermal efficiencies of the units. The parameters P_{P-L}^{t} and H_{P-L}^{t} also show the annual peak of electric and thermal load of the network.

2) Policy constraints related to the maximum capacity of the engine room unit, CHP, upstream network and the battery: These restrictions apply if the programmer intends to limit the capacity of the CHP, network, or battery. The lower limit of capacity is marked with the min index and the upper limit of capacity with the max index as follows;

$$S_{M\_min} \leq S_{M}^{t} \leq S_{M\_max} \quad (17)$$

$$S_{P-CHP\_min} \leq S_{P-CHP}^{t} \leq S_{P-CHP\_max} \quad (18)$$

$$S_{\text{buy}\_min} \leq S_{buy}^{t} \leq S_{\text{buy}\_max} \quad (19)$$

$$S_{\text{batt}\_min} \leq S_{batt}^{t} \leq S_{\text{batt}\_max} \quad (20)$$

It should be noted that the numerical bounds used in these equations are based on a combination of regulatory standards and engineering assumptions. Upper limits for grid exchange, battery capacity, and CHP sizing reflect national energy codes and infrastructure constraints typical of official buildings in Iran. Lower bounds are set to ensure minimum operational feasibility and avoid underutilization of installed systems. These values were validated through expert consultation and benchmarking against similar energy hub deployments.

3) Wind turbine constraint: In Equation (21), $S_{wind\_max}^{t}$ is the maximum power that can be extracted from the wind which depends on the weather conditions (wind speed) at the location of the hub (climate).

$$0 \leq S_{wind}^{t} \leq S_{wind\_max}^{t} \quad (21)$$

4) Geo thermal constraint: The extracted power of the geo thermal unit should be lower than its maximum power as presented in Eq. (22).

$$0 \leq S_{GT}^{t} \leq S_{GT\_max}^{t} \quad (22)$$

5) Photovoltaic constraint: This constraint, which is shown in Eq. (23), presents that produced power of the photovoltaic panel is lower than its maximum power. The maximum power is related to the solar irradiation and the weather conditions at the location of the energy hub.

$$0 \leq S_{pv}^{t} \leq S_{PV\_max}^{t} \quad (23)$$

6) Constraint of solar water heater: The available maximum power of solar water heater depends on the weather condition. So, its power should be lower than the maximum power as presented by Eq. (24).

$$0 \leq S_{solar}^{t} \leq S_{solar\_max}^{t} \quad (24)$$

7) Ground limit for equipment installation: The only space available for the installation of the solar panel and solar water heater is the roof space or a limited area. So, the amount of electrical power received in this space is limited. Therefore, Eq. (25) is considered to present that the total power of the solar units installed in this space should not be more than the predetermined value based on the location of energy hub.

$$S_{pv}^{t} + S_{solar}^{t} \leq E * Area \quad (25)$$

Where, E is the amount of energy received from the sun per square meter (depending on the climate of the energy hub) and the $Area$ of interest.

8) Policy constraints related to the minimum use of renewable resources: Equations (26) and (27) lead the model to make greater use of renewable sources to supply the hub with electrical and thermal power. They present that the capacity of the wind turbine and solar panel must be at least k_1 % of the electric charge and the hub capacity of the geothermal and solar water heater must be at least k_2 % of the thermal load.

$$S_{PV}^{t} + S_{wind}^{t} \geq k_1 * P_{L-max}^{t} \quad (26)$$

$$S_{solar}^{t} + S_{GT}^{t} \geq k_2 * H_{L-max}^{t} \quad (27)$$

9) Demand response policy constraint: The operator is allowed to cut off or transfer to a certain percentage of the electric P_{DR}^{t} and thermal H_{DR}^{t} peak loads, which are known as responsive loads, to reduce the amount of P_{L-max}^{t} and H_{L-max}^{t}. It causes to decrease the cost of programming. The number of responsive loads is one of the policy constraints of the system, as presented by equations (28) and (29).

$$P_{P-_L}^{t} = P_{L-max}^{t} - P_{DR}^{t} \quad (28)$$

$$H_{P-_L}^{t} = H_{L-max}^{t} - H_{DR}^{t} \quad (29)$$

3. Optimization algorithm

The main goal in this optimization is to find a set of solution to the objective function and including a set of linear constraints. In other words, the optimization problem is presented as follows [42-43];

Table 2 Area of different types of studied official buildings

Building type	Area (m^2)
T1	510.97
T2	2322.6
T3	4979.6
T4	46321.45

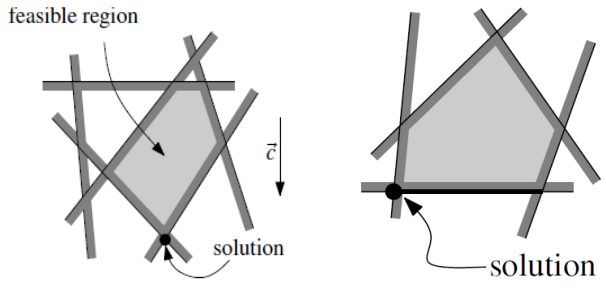

(a) (b)

Fig. 1 MILP programming (a: feasible region, b: optimal solution)

$$Maximize\ c_1x_1 + c_2x_2 + \cdots + c_dx_d \quad (30)$$

$$subject\ to \begin{cases} a_{11}x_1 + \cdots + a_{1d}x_d \le b_1 \\ \vdots \\ a_{11}x_1 + \cdots + a_{1d}x_d \le b_1 \end{cases} \quad (31)$$

The objective function can be considered as a directional vector. Figure 2 shows the method of applying MILP. As shown in this figure, $f_{\vec{c}}$ shows the objective function defined by the vector $\vec{C}$. To maximize the objective function, the farthest point must be found on the vector $\vec{C}$ in the feasible region. So, Equations (32) and (33) are considered.

$$\vec{C} = (C_x, C_y) \quad (32)$$

$$f_{\vec{C}}(p) = C_xP_x + C_yP_y \quad (33)$$

The CIPLEX method, which is widely and practically used in complex problems, is applied to solve the proposed problem. Therefore, the procedure is as follows:

1. The set of n linear constraints in a two-variable linear problem is denoted by $H = \{h_1, h_2, \ldots h_n\}$.
2. The vector $\vec{C}$ defines the objective function and the purpose is to fine a point in $p \in R^2$ where $f_{\vec{c}}$ is maximum and $p \in \cap H$.
3. The linear problem is represented by $(H, \vec{c})$ and the feasible region is marked with C.
4. Then, in each step, a constraint is added and an optimal solution is obtained for the new sub-problem. Therefore, the answer to each of the intermediate problems needs to be acceptable and unique. In other words, it is assumed that each intermediate feasible area has a unique optimal vertex, but this condition may not always be met. So, to ensure that the issue is finite, two new constraints are added as follows:

$$m_1 = \begin{cases} p_x \le M \ ; \ if\ c_x > 0 \\ -p_x \le M \ ; \ elsewhere \end{cases} \quad (34)$$

$$m_2 = \begin{cases} p_y \le M \ ; \ if\ c_y > 0 \\ -p_y \le M \ ; \ elsewhere \end{cases} \quad (35)$$

5. M must be large enough that the added constraints do not affect the optimal solutions, where m_1 and m_2 are selected independent to the half pages of the H. The subscription area of m_1 and m_2 regions is also a corner area. Therefore, if the infinite problem has an answer, in this case the smallest point in the lexical order will be the optimal point.
6. With these two conventions, every linear problem that becomes feasible has a unique answer, which is the vertex of the feasible region. This vertex is called the optimal vertex.
7. Therefore, the problem will be solved by repeating this loop.

4. Sensitivity analysis and simulation results

In this section, the proposed energy hub model is evaluated using real building case studies, and the simulation results are analyzed accordingly. The framework is applied to four distinct types of official buildings situated across various climatic zones in Iran. Areas of different buildings are listed in Table 2. Each of these buildings incorporates a combination of distributed energy resources, including photovoltaic panels, solar water heaters, wind turbines, storage units, a central heating plant with CHP capability, geothermal systems, and connections to the national electricity and gas networks. These components are coordinated by the energy hub to supply both electrical and thermal demands at minimum operational cost over the planning horizon [42].

To represent Iran's diverse environmental conditions, the study considers 12 climate zones. Each zone has unique temperature profile and energy load characteristics. The seasonal electrical and thermal demand profiles for these regions are illustrated in Fig. 3. The corresponding cities selected as pilot locations are Abadan (0B), Gachsaran (1A), Andimeshk (1B), Sepiddasht (2A), Fasa (2B), Amol (3A), Birjand (3B), Aligoudarz (4A), Arak (4B), Astara (4C), Maku (5A), and Ardabil (5C).

Table 3 The way of utilizing the output of solar water heaters in various cities of Iran

City (Climate zone)	The application of the output of solar water heaters	
	Hygienic use and indirect use for space heating	Direct use for space heating
Abadan (0B)	*	*
Gachsaran (1A)	*	*
Andimeshk (1B)	*	*
Sepiddasht (2A)	*	*
Fasa (2B)	*	*
Amol (3A)	*	*
Birjand (3B)	*	*
Aligoudarz (4A)	*	-
Arak (4B)	*	-
Astara (4C)	*	-
Maku (5A)	*	-
Ardabil (5C)	*	-

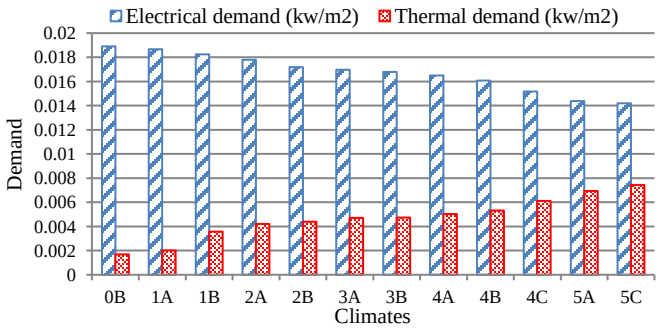

Fig. 2 Seasonal demand profiles for different climate regions

In the simulations, the cost of exchanging electricity with the upstream grid is assumed to be 9.5 cents per kilowatt-hour, and natural gas is priced at 13 cents per cubic meter. The nominal interest rate applied in financial modeling is set at 20 %. Because the optimization aligns with peak demand periods, some daily energy requirements may fall below maximum load levels. For this reason, battery capacity is conservatively sized at 30 % of the combined installed capacities of PV and wind energy systems to prevent excess generation from being wasted. These batteries are intended as reserve units and do not independently supply load. Under off-grid scenarios, the battery capacity is resized to 30 percent of either the diesel generator or PV output, maintaining its role as a reserve backup system [44]. All case study buildings are modeled as two-story structures. For the installation of PV arrays and solar thermal systems, the available rooftop area is calculated by dividing the total floor area by two, ensuring realistic spatial constraints for equipment placement. In terms of domestic hot water usage, operational limits for water temperature are defined based on sanitary and heating requirements. Water temperatures between 40°C and 50°C are suitable for hygienic use, whereas temperatures exceeding 50°C are applicable for space heating purposes. Given the variation in average ambient temperatures across the selected Iranian cities, Table 3 outlines optimized scenarios for deploying solar water heaters to meet these thermal thresholds effectively [44].

The management method is simulated under four scenarios to evaluate the performance and adaptability of the proposed energy hub framework. The scenarios are considered based on the different levels of renewable energy integration and operational flexibility. These scenarios are:

- Scenario 1: Zero renewable energy contribution
- Scenario 2: 50% renewable energy contribution
- Scenario 3: Full renewable energy deployment with diesel generator backup
- Scenario 4: Electricity export to the upstream grid

In the following, the results of applying the proposed energy hub are presented and its performance is evaluated in the presence of each scenario.

4.1. Scenario 1 - Zero renewable energy contribution

This baseline case models the energy hub using only conventional energy sources, such as grid electricity and natural gas, without any contribution from renewable systems. It reflects the traditional energy infrastructure typically seen in administrative buildings. Table 4 presents the optimal value of different components of the energy hub in this scenario.

Table 4 presents a description of the energy hub's behavior under Scenario 1, where no renewable energy sources are utilized. Across all twelve climatic zones and four building typologies, the model consistently relies on conventional energy carriers, namely grid electricity and boiler-based thermal generation, while showing zero utilization for renewable components such as PV panels, WTs, batteries, solar water heaters, geothermal systems, and CHP units. The grid electricity usage increases markedly with building scale, as seen in T1 through T4, illustrating proportional growth in energy demand with larger infrastructure footprints. For example, electricity demand ranges from about 9.3 kW for T1 buildings to over 875 kW for T4 buildings in hot climates such as Abadan (0B). Similarly, the capacity of boiler rooms intensifies in colder regions like Ardabil (5C), where the thermal demand necessitates up to 796 kW of boiler capacity in T4 structures.

The complete absence of PV, WT, and battery contribution reinforces the lack of energy self-sufficiency and highlights high operational dependency on fossil-based grid power.

Table 4 The optimal value of different components of the energy hub in different climates and buildings considering scenario 1

Building type and climate		Optimal power of different component (kW)							
City (Climate zone)	Building type	PV	WT	Battery	Solar water	Power network	Boiler room	Geo-thermal	CHP
Abadan (0B)	T1	0.00	0.00	0.00	0.00	9.65500	1.40700	0.00	0.00
	T2	0.00	0.00	0.00	0.00	43.8870	6.75900	0.00	0.00
	T3	0.00	0.00	0.00	0.00	94.0940	15.6520	0.00	0.00
	T4	0.00	0.00	0.00	0.00	875.286	180.987	0.00	0.00
Gachsaran (1A)	T1	0.00	0.00	0.00	0.00	9.53400	1.66600	0.00	0.00
	T2	0.00	0.00	0.00	0.00	43.3380	8.00600	0.00	0.00
	T3	0.00	0.00	0.00	0.00	92.9170	18.5390	0.00	0.00
	T4	0.00	0.00	0.00	0.00	864.334	214.368	0.00	0.00
Andimeshk (1B)	T1	0.00	0.00	0.00	0.00	9.32800	2.96700	0.00	0.00
	T2	0.00	0.00	0.00	0.00	42.4000	14.2550	0.00	0.00
	T3	0.00	0.00	0.00	0.00	90.9060	33.0110	0.00	0.00
	T4	0.00	0.00	0.00	0.00	845.631	381.714	0.00	0.00
Sepiddasht (2A)	T1	0.00	0.00	0.00	0.00	9.08700	3.50400	0.00	0.00
	T2	0.00	0.00	0.00	0.00	41.3030	16.8350	0.00	0.00
	T3	0.00	0.00	0.00	0.00	88.5550	38.9840	0.00	0.00
	T4	0.00	0.00	0.00	0.00	823.756	450.778	0.00	0.00
Fasa (2B)	T1	0.00	0.00	0.00	0.00	8.78000	3.67100	0.00	0.00
	T2	0.00	0.00	0.00	0.00	39.9100	17.6360	0.00	0.00
	T3	0.00	0.00	0.00	0.00	85.5670	40.8380	0.00	0.00
	T4	0.00	0.00	0.00	0.00	795.963	472.223	0.00	0.00
Amol (3A)	T1	0.00	0.00	0.00	0.00	8.67800	3.92100	0.00	0.00
	T2	0.00	0.00	0.00	0.00	39.4450	18.8370	0.00	0.00
	T3	0.00	0.00	0.00	0.00	84.5710	43.6200	0.00	0.00
	T4	0.00	0.00	0.00	0.00	786.699	504.391	0.00	0.00
Birjand (3B)	T1	0.00	0.00	0.00	0.00	8.57600	3.93800	0.00	0.00
	T2	0.00	0.00	0.00	0.00	38.9810	18.9170	0.00	0.00
	T3	0.00	0.00	0.00	0.00	83.5750	43.8060	0.00	0.00
	T4	0.00	0.00	0.00	0.00	777.435	506.535	0.00	0.00
Aligoudarz (4A)	T1	0.00	0.00	0.00	0.00	8.42300	4.18800	0.00	0.00
	T2	0.00	0.00	0.00	0.00	38.2840	20.1180	0.00	0.00
	T3	0.00	0.00	0.00	0.00	82.0810	46.5880	0.00	0.00
	T4	0.00	0.00	0.00	0.00	763.538	538.703	0.00	0.00
Arak (4B)	T1	0.00	0.00	0.00	0.00	8.21800	4.43800	0.00	0.00
	T2	0.00	0.00	0.00	0.00	37.3550	21.3200	0.00	0.00
	T3	0.00	0.00	0.00	0.00	80.0890	49.3700	0.00	0.00
	T4	0.00	0.00	0.00	0.00	745.010	570.870	0.00	0.00
Astara (4C)	T1	0.00	0.00	0.00	0.00	7.75800	5.10500	0.00	0.00
	T2	0.00	0.00	0.00	0.00	35.2650	24.5230	0.00	0.00
	T3	0.00	0.00	0.00	0.00	75.6080	56.7880	0.00	0.00
	T4	0.00	0.00	0.00	0.00	703.320	656.651	0.00	0.00
Maku (5A)	T1	0.00	0.00	0.00	0.00	7.35000	5.77200	0.00	0.00
	T2	0.00	0.00	0.00	0.00	33.4070	27.7270	0.00	0.00
	T3	0.00	0.00	0.00	0.00	71.6240	64.2060	0.00	0.00
	T4	0.00	0.00	0.00	0.00	666.263	742.431	0.00	0.00
Ardabil (5C)	T1	0.00	0.00	0.00	0.00	7.24700	6.18800	0.00	0.00
	T2	0.00	0.00	0.00	0.00	32.9420	29.7290	0.00	0.00
	T3	0.00	0.00	0.00	0.00	70.6280	68.8430	0.00	0.00
	T4	0.00	0.00	0.00	0.00	656.999	796.044	0.00	0.00

In this scenario, the CHP and geothermal systems are not activated, reflecting either policy constraints or the model's prioritization of more readily available sources to meet cost optimization criteria. This centralized supply pattern indicates a conventional strategy where resilience and sustainability are compromised in favor of reliability and simplicity. While sufficient for uninterrupted power delivery, this setup exposes the buildings to heightened risks related to energy price volatility, emissions penalties, and vulnerability during supply disruptions. The scenario establishes a baseline against which the advantages of renewable integration and distributed generation will be compared in subsequent simulations.

4.2. Scenario 2 - 50% renewable energy contribution

In this intermediate scenario, renewable energy systems including photovoltaic panels, wind turbines, and geothermal resources are configured to supply half of the building's total energy demand. This setup tests the hub's ability to coordinate mixed energy carriers while reducing reliance on fossil fuels. The optimal value of different components of the energy hub in this scenario is presented in Table 5.

Table 5 illustrates the simulation results for Scenario 2, where the energy hub is designed to supply 50% of the total building demand using renewable energy sources. Across all cities and building typologies, a balanced co-existence between renewables and conventional sources is observed. In this configuration, PV systems are the primary renewable contributors, showing consistent deployment across all climates and scales. For instance, PV power ranges from about 3.6 kW in Ardabil′s small-scale buildings (T1) to approximately

Table 5 The optimal value of different components of the energy hub in different climates and buildings considering scenario 2

Building type and climate		Optimal power of different component (kW)							
City (Climate zone)	Building type	PV	WT	Battery	Solar water	Power network	Boiler room	Geo-thermal	CHP
Abadan (0B)	T1	4.82800	0.00	1.44800	0.70400	4.82800	0.70300	0.00	0.00
	T2	21.9440	0.00	6.58300	3.37900	21.9440	3.38000	0.00	0.00
	T3	47.0470	0.00	14.1140	7.82600	47.0470	7.82600	0.00	0.00
	T4	437.643	0.00	131.293	90.4930	437.643	90.4940	0.00	0.00
Gachsaran (1A)	T1	4.76700	0.00	1.43000	0.83300	4.76700	0.83300	0.00	0.00
	T2	21.6690	0.00	6.50100	4.00300	21.6690	4.00300	0.00	0.00
	T3	46.4580	0.00	13.9380	9.27000	46.4580	9.26900	0.00	0.00
	T4	432.167	0.00	129.650	107.184	432.167	107.184	0.00	0.00
Andimeshk (1B)	T1	4.66400	0.00	1.39900	1.48300	4.66400	1.48400	0.00	0.00
	T2	21.2000	0.00	6.36000	7.12700	21.2000	7.12800	0.00	0.00
	T3	45.4530	0.00	13.6360	16.5050	45.4530	16.5060	0.00	0.00
	T4	422.816	0.00	126.845	190.857	422.816	190.857	0.00	0.00
Sepiddasht (2A)	T1	4.54300	0.00	1.36300	1.75200	4.54300	1.75200	0.00	0.00
	T2	20.6520	0.00	6.19600	8.41800	20.6520	8.41700	0.00	0.00
	T3	44.2770	0.00	13.2830	19.4920	44.2770	19.4920	0.00	0.00
	T4	411.878	0.00	123.563	225.389	411.878	225.389	0.00	0.00
Fasa (2B)	T1	4.39000	0.00	1.31700	1.83600	4.39000	1.83500	0.00	0.00
	T2	19.9550	0.00	5.98600	8.81800	19.9550	8.81800	0.00	0.00
	T3	42.7830	0.00	12.8350	20.4190	42.7830	20.4190	0.00	0.00
	T4	397.982	0.00	119.395	236.112	397.982	236.111	0.00	0.00
Amol (3A)	T1	4.33900	0.00	1.30200	1.96000	4.33900	1.96100	0.00	0.00
	T2	19.7230	0.00	5.91700	9.41900	19.7230	9.41800	0.00	0.00
	T3	42.2850	0.00	12.6860	21.8100	42.2850	21.8100	0.00	0.00
	T4	393.350	0.00	118.005	252.196	393.350	252.195	0.00	0.00
Birjand (3B)	T1	4.28800	0.00	1.28600	1.96900	4.28800	1.96900	0.00	0.00
	T2	19.4900	0.00	5.84700	9.45900	19.4900	9.45800	0.00	0.00
	T3	41.7870	0.00	12.5360	21.9030	41.7870	21.9030	0.00	0.00
	T4	388.717	0.00	116.615	253.267	388.717	253.268	0.00	0.00
Aligoudarz (4A)	T1	4.21100	0.00	1.26300	2.09400	4.21100	2.09400	0.00	0.00
	T2	19.1420	0.00	5.74300	10.0590	19.1420	10.0590	0.00	0.00
	T3	41.0410	0.00	12.3120	23.2940	41.0410	23.2940	0.00	0.00
	T4	381.769	0.00	114.531	269.352	381.769	269.351	0.00	0.00
Arak (4B)	T1	4.10900	0.00	1.23300	2.21900	4.10900	2.21900	0.00	0.00
	T2	18.6770	0.00	5.60300	10.6600	18.6770	10.6600	0.00	0.00
	T3	40.0450	0.00	12.0130	24.6850	40.0450	24.6850	0.00	0.00
	T4	372.505	0.00	111.751	285.435	372.505	285.435	0.00	0.00
Astara (4C)	T1	3.87900	0.00	1.16400	2.55300	3.87900	2.55200	0.00	0.00
	T2	17.6320	0.00	5.29000	12.2610	17.6320	12.2620	0.00	0.00
	T3	37.8040	0.00	11.3410	28.3940	37.8040	28.3940	0.00	0.00
	T4	351.660	0.00	105.498	328.326	351.660	328.325	0.00	0.00
Maku (5A)	T1	3.67500	0.00	1.10200	2.88600	3.67500	2.88600	0.00	0.00
	T2	16.7030	0.00	5.01100	13.8640	16.7030	13.8630	0.00	0.00
	T3	35.8120	0.00	10.7440	32.1030	35.8120	32.1030	0.00	0.00
	T4	333.132	0.00	99.9390	371.215	333.132	371.216	0.00	0.00
Ardabil (5C)	T1	3.62400	0.00	1.08700	3.09400	3.62400	3.09400	0.00	0.00
	T2	16.4710	0.00	4.94100	14.8650	16.4710	14.8640	0.00	0.00
	T3	35.3140	0.00	10.5940	34.4220	35.3140	34.4210	0.00	0.00
	T4	328.500	0.00	98.5500	398.022	328.500	398.022	0.00	0.00

437 kW in Abadan′s largest typology (T4). Wind turbines, however, are not activated in any region, likely due to localized wind limitations or unfavorable economic thresholds in the optimization. Notably, battery systems emerge with significant capacities, roughly 30% of the corresponding PV values, supporting energy storage and improving dispatch flexibility, particularly during peak load hours or limited grid availability.

Solar water heaters are actively utilized, with their contribution scaled according to local solar thermal potential and thermal load demand. Warmer zones such as Abadan and Gachsaran show comparatively smaller water heater capacities, while colder regions like Ardabil and Maku reflect larger installations—indicating climate-responsive deployment. Interestingly, grid electricity is still retained in this hybrid setup, mirroring PV contributions almost exactly, suggesting symmetrical load sharing between local generation and external supply. This dual reliance enhances resilience while lowering operational costs relative to Scenario 1.

Across all entries, boiler rooms continue to serve residual thermal loads, though at significantly reduced capacity compared to the baseline case. Components like geothermal and CHP systems remain inactive, possibly due to design constraints, limited resource availability, or model prioritization favoring PV and solar thermal technologies. Overall, Scenario 2 demonstrates a pragmatic integration of renewable energy, achieving cost-effective and environmentally beneficial operation while maintaining system stability. The results confirm that even partial renewable adoption leads to substantial performance improvements in official buildings across diverse Iranian climates.

Table 3 The optimal value of different components of the energy hub in different climates and buildings considering scenario 3

Building type and climate		Optimal power of different component (kW)							
City (Climate zone)	Building type	PV	WT	Battery	Solar water	Power network	Boiler room	Geo-thermal	CHP
Abadan (0B)	T1	0.00	0.00	2.89650	0.60782	0.00	0.00	0.00	0.00
	T2	0.00	0.00	13.1660	2.91989	0.00	0.00	0.00	0.00
	T3	0.00	0.00	28.2280	6.76166	0.00	0.00	0.00	0.00
	T4	0.00	0.00	262.586	78.1864	0.00	0.00	0.00	0.00
Gachsaran (1A)	T1	0.00	0.00	2.86020	0.71971	0.00	0.00	0.00	0.00
	T2	0.00	0.00	13.0014	3.45859	0.00	0.00	0.00	0.00
	T3	0.00	0.00	27.8751	8.00885	0.00	0.00	0.00	0.00
	T4	0.00	0.00	259.300	92.6070	0.00	0.00	0.00	0.00
Andimeshk (1B)	T1	0.00	0.00	2.79840	1.28174	0.00	0.00	0.00	0.00
	T2	0.00	0.00	12.7200	6.15816	0.00	0.00	0.00	0.00
	T3	0.00	0.00	27.2718	14.2608	0.00	0.00	0.00	0.00
	T4	0.00	0.00	253.689	164.901	0.00	0.00	0.00	0.00
Sepiddasht (2A)	T1	0.00	0.00	2.72610	1.51373	0.00	0.00	0.00	0.00
	T2	0.00	0.00	12.3909	7.27272	0.00	0.00	0.00	0.00
	T3	0.00	0.00	26.5665	16.8411	0.00	0.00	0.00	0.00
	T4	0.00	0.00	247.127	194.736	0.00	0.00	0.00	0.00
Fasa (2B)	T1	0.00	0.00	2.63400	1.58587	0.00	0.00	0.00	0.00
	T2	0.00	0.00	11.9730	7.61875	0.00	0.00	0.00	0.00
	T3	0.00	0.00	25.6701	17.6420	0.00	0.00	0.00	0.00
	T4	0.00	0.00	238.789	204.001	0.00	0.00	0.00	0.00
Amol (3A)	T1	0.00	0.00	2.60340	1.69387	0.00	0.00	0.00	0.00
	T2	0.00	0.00	11.8335	8.13758	0.00	0.00	0.00	0.00
	T3	0.00	0.00	25.3713	18.8438	0.00	0.00	0.00	0.00
	T4	0.00	0.00	236.010	217.897	0.00	0.00	0.00	0.00
Birjand (3B)	T1	0.00	0.00	2.57280	1.70122	0.00	0.00	0.00	0.00
	T2	0.00	0.00	11.6943	8.17214	0.00	0.00	0.00	0.00
	T3	0.00	0.00	25.0725	18.9242	0.00	0.00	0.00	0.00
	T4	0.00	0.00	233.231	218.823	0.00	0.00	0.00	0.00
Aligoudarz (4A)	T1	0.00	0.00	2.52690	1.80922	0.00	0.00	0.00	0.00
	T2	0.00	0.00	11.4852	8.69098	0.00	0.00	0.00	0.00
	T3	0.00	0.00	24.6243	20.1260	0.00	0.00	0.00	0.00
	T4	0.00	0.00	229.062	232.720	0.00	0.00	0.00	0.00
Arak (4B)	T1	0.00	0.00	2.46540	1.91722	0.00	0.00	0.00	0.00
	T2	0.00	0.00	11.2065	9.21024	0.00	0.00	0.00	0.00
	T3	0.00	0.00	24.0267	21.3279	0.00	0.00	0.00	0.00
	T4	0.00	0.00	223.503	246.616	0.00	0.00	0.00	0.00
Astara (4C)	T1	0.00	0.00	2.32740	2.20536	0.00	0.00	0.00	0.00
	T2	0.00	0.00	10.5795	10.5939	0.00	0.00	0.00	0.00
	T3	0.00	0.00	22.6824	24.5324	0.00	0.00	0.00	0.00
	T4	0.00	0.00	210.996	283.673	0.00	0.00	0.00	0.00
Maku (5A)	T1	0.00	0.00	2.20500	2.49351	0.00	0.00	0.00	0.00
	T2	0.00	0.00	10.0221	11.9781	0.00	0.00	0.00	0.00
	T3	0.00	0.00	21.4872	27.7370	0.00	0.00	0.00	0.00
	T4	0.00	0.00	199.879	320.730	0.00	0.00	0.00	0.00
Ardabil (5C)	T1	0.00	0.00	2.17410	2.67322	0.00	0.00	0.00	0.00
	T2	0.00	0.00	9.88260	12.8429	0.00	0.00	0.00	0.00
	T3	0.00	0.00	21.1884	29.7402	0.00	0.00	0.00	0.00
	T4	0.00	0.00	197.010	343.891	0.00	0.00	0.00	0.00

4.3. Scenario 3 - Full renewable energy deployment with diesel generator backup

This scenario assumes 100% of the energy demand is met by renewable sources. To ensure operational reliability, especially during intermittency or outages, a diesel generator is added to serve as an emergency backup. In this scenario, the energy hub is assumed to operate in a remote area disconnected from the main electricity grid, where extending transmission infrastructure is economically or technically unfeasible. As a result, a diesel generator is introduced to fully substitute the upstream electricity supply. Additionally, due to the absence of a centralized natural gas network, thermal energy cannot be economically sourced through conventional means. Therefore, solar water heaters are assigned the responsibility of meeting the building's thermal requirements.

The energy demand of the buildings is assumed to be fully met by the diesel generator, which is prioritized due to its lower investment and operational costs compared to photovoltaic and wind technologies under isolated grid conditions. To enhance reliability, 30% of the diesel-generated electrical power is stored in battery systems, functioning as reserve capacity. Table 6 presents the optimal capacities of various energy hub components across different building types and climate zones. The results presented in Table 6 provide insights into the operation of the energy hub under Scenario 3, where the system is completely off-grid and reliant on diesel generators and solar water heaters, due to the unavailability of both electricity and natural gas networks.

In all climatic zones and building types, renewable electrical

sources such as PV and WT are absent, reinforcing the model's prioritization of diesel generation as the sole power supply-driven by its lower capital cost and higher availability in isolated areas. Diesel generator capacities scale with building size and climate-induced load; for instance, they range from approximately 7 kW in Ardabil's smallest buildings to nearly 875 kW in Abadan′s largest (T4), clearly reflecting growing demand with infrastructure expansion and warmer climates.

Correspondingly, battery systems are activated across all cases, sized to about 30% of the diesel generator's output, confirming their role as backup reserves to mitigate reliability risks and energy variability. Solar water heaters are the only thermal generation units employed, with capacities adjusted for regional solar thermal potential and sanitary heating needs. Cold-climate zones such as Maku and Ardabil show higher deployment, exceeding 300 kW in T4 buildings, while southern zones like Abadan and Gachsaran maintain modest installations under 100 kW. Notably, none of the conventional components, including grid connection, boiler room, CHP, or geothermal systems, are activated, highlighting the simplicity and localized focus of the off-grid configuration.

This scenario emphasizes survival-oriented energy planning for maximizing availability over efficiency. While it offers complete autonomy, the reliance on diesel introduces high operational costs and substantial emissions. However, in strategic contexts where grid access is infeasible and passive defense criteria dominate, this setup demonstrates a practical and minimally invasive energy provision model for remote official infrastructure.

Table 7 The optimal value of different components of the energy hub in different climates and buildings considering scenario 4

Building type and climate		Optimal power of different component (kW)							
City (Climate zone)	Building type	PV	WT	Battery	Solar water	Power network	Boiler room	Geo-thermal	CHP
Abadan (0B)	T1	1.9310	0.00	0.5790	0.2810	7.7240	1.1260	0.00	0.000
	T2	8.7770	0.00	2.6330	1.3520	35.110	5.4070	0.00	0.000
	T3	18.819	0.00	5.6460	3.1300	75.275	12.522	0.00	0.000
	T4	152.42	0.00	45.620	19.910	712.44	161.07	0.00	201.33
Gachsaran (1A)	T1	1.9070	0.00	0.5720	0.3330	7.6280	1.3330	0.00	0.000
	T2	8.6680	0.00	2.6000	1.6010	34.670	6.4050	0.00	0.000
	T3	18.583	0.00	5.5750	3.7080	74.333	14.831	0.00	0.000
	T4	148.52	0.00	44.560	23.580	705.11	190.78	0.00	198.22
Andimeshk (1B)	T1	1.8660	0.00	0.5600	0.5930	7.4620	2.3740	0.00	0.000
	T2	8.4800	0.00	2.5440	2.8510	33.920	11.404	0.00	0.000
	T3	18.181	0.00	5.4540	6.6020	72.725	26.409	0.00	0.000
	T4	143.52	0.00	43.056	41.990	692.55	339.72	0.00	194.55
Sepiddasht (2A)	T1	1.8170	0.00	0.5450	0.7010	7.2690	2.8030	0.00	0.000
	T2	8.2610	0.00	2.4780	3.3670	33.043	13.468	0.00	0.000
	T3	17.711	0.00	5.3130	7.7970	70.844	31.187	0.00	0.000
	T4	139.85	0.00	41.955	49.880	674.55	401.19	0.00	189.52
Fasa (2B)	T1	1.7560	0.00	0.5270	0.7340	7.0240	2.9370	0.00	0.000
	T2	7.9820	0.00	2.3950	3.5280	31.928	14.108	0.00	0.000
	T3	17.113	0.00	5.1340	8.1670	68.453	32.671	0.00	0.000
	T4	135.55	0.00	40.665	51.950	651.22	420.27	0.00	183.02
Amol (3A)	T1	1.7360	0.00	0.5210	0.7840	6.9420	3.1370	0.00	0.000
	T2	7.8890	0.00	2.3670	3.7670	31.556	15.070	0.00	0.000
	T3	16.914	0.00	5.0740	8.7240	67.657	34.896	0.00	0.000
	T4	131.02	0.00	39.306	55.490	646.95	448.90	0.00	180.06
Birjand (3B)	T1	1.7150	0.00	0.5150	0.7880	6.8610	3.1500	0.00	0.000
	T2	7.7960	0.00	2.3390	3.7830	31.185	15.134	0.00	0.000
	T3	16.715	0.00	5.0140	8.7610	66.860	35.045	0.00	0.000
	T4	128.75	0.00	38.625	55.720	639.85	450.81	0.00	178.25
Aligoudarz (4A)	T1	1.6850	0.00	0.5050	0.8380	6.7380	3.3500	0.00	0.000
	T2	1.6850	0.00	2.2970	4.0230	30.627	16.095	0.00	0.000
	T3	16.416	0.00	4.9250	9.3180	65.665	37.270	0.00	0.000
	T4	124.32	0.00	37.296	59.260	630.25	479.44	0.00	175.66
Arak (4B)	T1	1.6440	0.00	0.4930	0.8880	6.5750	3.5500	0.00	0.000
	T2	7.4710	0.00	2.2410	4.2640	29.884	17.056	0.00	0.000
	T3	16.018	0.00	4.8050	9.8740	64.071	39.496	0.00	0.000
	T4	119.99	0.00	35.997	62.850	616.25	508.07	0.00	171.24
Astara (4C)	T1	1.5520	0.00	0.4650	1.0210	6.2070	4.0840	0.00	0.000
	T2	7.0530	0.00	2.1160	4.9040	28.212	19.619	0.00	0.000
	T3	15.122	0.00	4.5360	11.358	60.486	45.430	0.00	0.000
	T4	116.22	0.00	34.866	72.240	579.52	584.41	0.00	161.58
Maku (5A)	T1	1.4700	0.00	0.4410	1.1550	5.8800	4.6170	0.00	0.000
	T2	6.6810	0.00	2.0040	5.5460	26.725	22.181	0.00	0.000
	T3	14.325	0.00	4.2970	12.841	57.299	51.365	0.00	0.000
	T4	112.62	0.00	33.786	81.680	545.52	660.74	0.00	153.94
Ardabil (5C)	T1	1.4490	0.00	0.4350	1.2370	5.7980	4.9510	0.00	0.000
	T2	6.5880	0.00	1.9770	5.9460	26.354	23.783	0.00	0.000
	T3	14.126	0.00	4.2380	13.769	56.502	55.074	0.00	0.000
	T4	108.85	0.00	108.85	87.290	540.65	708.75	0.00	151.42

4.4. Scenario 4 - Electricity export to the main grid

In the final scenario, the energy hub is granted permission to sell surplus electricity to the upstream network. This market-oriented approach explores the financial and technical impact of bidirectional energy exchange, potentially transforming the building from a passive consumer into an active participant in the energy market. In this scenario, the energy hub is modeled under the assumption that electricity generation exceeds on-site consumption, enabling the possibility of exporting surplus power to the upstream grid. The task of electricity production is assigned to the combined heat and power unit, which is fully activated to generate exportable capacity. For CHP to be selected within the simulation framework, its investment cost must remain competitive with other technologies such as photovoltaic panels, wind turbines, and batteries. Under these conditions, the simulation reveals a hybrid supply strategy, electricity is generated by both the upstream grid and the CHP unit, while thermal demand is met solely by boiler systems. The optimal value of different components of the energy hub in this scenario is presented in Table 7.

Table 7 show that CHP units are selected exclusively in locations with Type 4 buildings, where energy demand justifies higher generation and export capacity. In these cases, CHP systems supply approximately 23% of total electrical demand and 11% of total thermal demand across the modeled regions. To reach the investment break-even point, the energy hub must sell at least 18% of its total electricity generation to the upstream grid. This scenario highlights the financial and operational viability of electricity market participation for large administrative buildings and demonstrates how strategic export policies can enhance the economic performance of multi-energy systems. In this configuration, combined heat and power (CHP) units are selectively deployed to generate surplus electricity for sale, contingent on their competitiveness with other technologies such as PV, wind, and batteries. The results reveal that CHP units are only installed in buildings of Type 4, which represent the largest administrative typology with the highest energy demands. Their capacities vary by climate zone, reaching as high as 201.33 kW in Abadan, and averaging around 175–195 kW across cooler regions such as Gachsaran, Arak, and Ardabil. This targeted deployment reflects both load justification and profitability potential, as these buildings can sustain CHP investment and achieve exportable surplus.

Across all regions and building sizes, photovoltaic panels are present, with capacities increasing proportionally to building scale and solar availability. For instance, PV power reaches 152.42 kW in Abadan (T4), while remaining modest in cooler regions like Ardabil (around 108.85 kW in T4). However, wind turbines are entirely absent, suggesting limited wind resource feasibility or economic advantage under current cost assumptions. Battery systems are consistently used, primarily to buffer PV and CHP output and facilitate timed electricity export; their sizing reflects building scale, reaching nearly 46 kW in some southern zones.

Solar water heaters show strong deployment across all cities, with capacity intensifying in colder climates (e.g., 87.29 kW in Ardabil′s T4 buildings) to meet both sanitary and heating demands. Meanwhile, boiler rooms are used extensively as the primary thermal source, especially where CHP thermal output is insufficient or absent. Notably, CHP contributes approximately 23% of total electrical demand and 11% of thermal demand in buildings where it is deployed. From a profitability standpoint, the system is designed so that 18% of total electricity generation is exported, enabling the hub to reach its investment break-even point.

Totally, Scenario 4 showcases a hybrid energy strategy that balances internal consumption and grid interaction. By leveraging CHP and PV technologies for both supply and export, the hub transitions into a proactive market participant, offering economic and operational benefits tailored to large-scale official buildings. This configuration underscores the value of targeted CHP deployment and flexible energy

management in driving profitability and resilience across diverse climate zones.

5. Conclusion

This study presented a sensitivity-based optimization framework for multi-carrier energy systems tailored to official buildings, aiming to minimize operational costs and enhance profitability from the perspective of an energy hub operator. Results across twelve climatic zones and four building typologies in Iran demonstrate that system performance is highly sensitive to input availability, cost structures, and policy constraints. In Scenario 1, where no renewable sources were used, operational reliance on grid electricity and gas led to the highest energy cost, with building Type 4 in Ardabil requiring up to 796 kW of boiler capacity and nearly 657 kW of grid electricity. In contrast, Scenario 2 enabled 50% renewable penetration, reducing grid dependency by half while solar water heater usage rose substantially (e.g., 398 kW in Ardabil). Scenario 3, operating off-grid with diesel generation, revealed that batteries sized at 30% of diesel capacity are essential for reliability but increase capital costs. CHP deployment in Scenario 4, limited to Type 4 buildings, supplied 23% of total electricity and 11% of thermal demand, with 18% of generated electricity sold to the grid to reach financial breakeven. The results presented that distributed generation is economically unattractive unless grid tariffs rise or investment costs decline. Moreover, a trade-off between boilers and electric heaters is necessary to balance thermal supply against the cost of gas and electricity. On the other hand, CHP units can contribute to cost reduction when allowed to export electricity, especially in high-demand typologies. In addition, participation in forward electricity markets can significantly lower planning costs, provided contract risk is managed appropriately. Also, batteries enhance system reliability but require careful sizing, considering parameters like depth of discharge and regional load profiles. For future research, it is recommended to examine the impact of multi-energy systems on power system reliability and to explore optimal design and operation of microgrids incorporating integrated energy hubs under dynamic market and resilience constraints.

References

[1] R. Hamzeh and M. Narimani, "Review, Definition and Challenges of Electrical Energy Hubs," arXiv preprint, arXiv:2504.06373, Apr. 2025.

[2] Y. Ghasemi, M. Khodabakhsh, and B. Sheikhi, "Energy Management of Energy Hub with Renewable Energy Resources Based on GTOA-ACNN Approach," *Environment, Development and Sustainability*, vol. 27, no. 3, pp. 10549–10574, 2025.

[3] A. Tavakkoli and S. H. Hosseini, "Coupling Energy Management of Power Systems with Energy Hubs through TSO-DSO Coordination," *International Journal of Electrical and Electronic Power Systems*, vol. 12, no. 1, pp. 34–45, Jan. 2024.

[4] S. Moradi and F. Akhlaghi, "Optimal Operation of Energy Hub-Based Microgrids with Intermittent RESs and Multi-type Energy Storage Systems," *Energy Systems*, vol. 16, no. 2, pp. 289–309, Mar. 2024.

[5] Sadi, S., et al., Classification of Energy Consumption of Lighting System in Buildings: a New Method, *Iranian Journal of Energy*, vol. 24, pp. 7-33, 2021.

[6] H. Esmaili, M. Jannati, and R. Teymouri, "Optimal Operation of Energy Hubs Integrated with Electric Vehicles, Load Management, Combined Heat and Power Unit and Renewable Energy Sources," *Farda Paper Technical Reports*, Jan. 2025.

[7] R. Ebrahimi and A. Kiani, "Technical and Economic Energy Optimization of the Energy Hub System Considering Peak Demand Pricing," *Energy, Ecology and Environment*, vol. 10, pp. 112–127, Feb. 2024.

[8] Sadi, S., et al., "Electrical Energy Saving in Office Equipments: Life Cycle Cost Method", *Iranian Journal of Energy*, vol. 24, pp. 101-134, 2021.

[9] T. Zhang, Y. Zhou, and L. Huang, "Stochastic Optimization for Minimizing Operational Costs in Smart Hybrid Energy Networks Considering Electric Vehicle," *PLoS ONE*, vol. 20, no. 1, pp. e0323491, Jan. 2025.

[10] H. Ren, W. Zhou, K. I. Nakagami, W. Gao, and Q. Wu, "Multi-objective optimization for the operation of distributed energy systems considering economic and environmental aspects," *Applied Energy*, vol. 87, no. 12, pp. 3642–3651, Dec. 2010.

[11] H. Ren and W. Gao, "A MILP model for integrated plan and evaluation of distributed energy systems," *Applied Energy*, vol. 87, no. 3, pp. 1001–1014, Mar. 2010.

[12] M. C. Bozchalui and R. Sharma, "Optimal operation of commercial building microgrids using multi-objective optimization to achieve emissions and efficiency targets," *in Proc. IEEE PES General Meeting*, San Diego, CA, USA, Jul. 2012, pp. 1–8.

[13] J. S. Kim and T. F. Edgar, "Optimal scheduling of combined heat and power plants using mixed-integer nonlinear programming," *Energy*, vol. 77, pp. 675–690, Dec. 2014.

[14] H. Wang, W. Yin, E. Abdollahi, R. Lahdelma, and W. Jiao, "Modelling and optimization of CHP based district heating system with renewable energy production and energy storage," *Applied Energy*, vol. 159, pp. 401–421, Dec. 2015.

[15] C. Marnay et al., "Optimal technology selection and operation of commercial-building microgrids," *IEEE Trans. Power Syst*., vol. 23, no. 3, pp. 975–982, Aug. 2008.

[16] K. K. Shah, A. S. Mundada, and J. M. Pearce, "Performance of U.S. hybrid distributed energy systems: Solar photovoltaic, battery and combined heat and power," *Energy Convers. Manage*., vol. 105, pp. 71–80, Nov. 2015.

[17] T. Sousa, H. Morais, J. Soares, and Z. Vale, "Day-ahead resource scheduling in smart grids considering Vehicle-to-Grid and network constraints," *Applied Energy*, vol. 96, pp. 183–193, Aug. 2012.

[18] F. Basrawi, T. Yamada, and S. Y. Obara, "Economic and environmental based operation strategies of a hybrid photovoltaic–microgas turbine trigeneration system," *Applied Energy*, vol. 121, pp. 174–183, May 2014.

[19] A. H. Nosrat, L. G. Swan, and J. M. Pearce, "Improved performance of hybrid photovoltaic-trigeneration systems over photovoltaic-cogen systems including effects of battery storage," *Energy*, vol. 49, pp. 366–374, Jan. 2013.

[20] X. Hu, L. Johannesson, N. Murgovski, and B. Egardt, "Longevity-conscious dimensioning and power management of the hybrid energy storage system in a fuel cell hybrid electric bus," *Applied Energy*, vol. 137, pp. 913–924, Jan. 2015.

[21] M. Moeini-Aghtaie, A. Abbaspour, M. Fotuhi-Firuzabad, and E. Hajipour, "A decomposed solution to multiple-energy carriers optimal power flow," *IEEE Trans. Power Syst*., vol. 29, no. 2, pp. 707–716, Mar. 2014.

[22] M. Moeini-Aghtaie, P. Dehghanian, M. Fotuhi-Firuzabad, and A. Abbaspour, "Multiagent genetic algorithm: An online probabilistic view on economic dispatch of energy hubs constrained by wind availability," *IEEE Trans. Sustain. Energy*, vol. 5, no. 2, pp. 699–708, Apr. 2014.

[23] A. Parisio, C. Del Vecchio, and A. Vaccaro, "A robust optimization approach to energy hub management," *Int. J. Electr. Power Energy Syst*., vol. 42, no. 1, pp. 98–104, Nov. 2012.

[24] F. Kienzle and G. Andersson, "Valuing investments in multi-energy conversion, storage, and demand-side management systems under uncertainty," *IEEE Trans. Sustain. Energy*, vol. 2,

no. 2, pp. 194–202, Apr. 2011.
[25] S. Pazouki, M.-R. Haghifam, and A. Moser, "Uncertainty modeling in optimal operation of energy hub in presence of wind, storage and demand response," *Int. J. Electr. Power Energy Syst.*, vol. 61, pp. 335–345, Oct. 2014.
[26] M. Moeini-Aghtaie, A. Abbaspour, and M. Fotuhi-Firuzabad, "Online multi criteria framework for charging management of PHEVs," *IEEE Trans. Veh. Technol*., vol. 63, no. 7, pp. 3028–3037, Sept. 2014.
[27] A. Parisio, C. Del Vecchio, and A. Vaccaro, "A robust optimization approach to energy hub management," *Int. J. Electr. Power Energy Syst*., vol. 42, no. 1, pp. 98–104, Nov. 2012.
[28] R. Evins, K. Orehounig, V. Dorer, and J. Carmeliet, "New formulations of the 'energy hub' model to address operational constraints," *Energy*, vol. 73, pp. 387–398, Aug. 2014.
[29] M. Rastegar and M. Fotuhi-Firuzabad, "Load management in a residential energy hub with renewable distributed energy resources," *Energy Build*., vol. 107, pp. 234–242, Oct. 2015.
[30] A. Sheikhi, S. Bahrami, and A. M. Ranjbar, "An autonomous demand response program for electricity and natural gas networks in smart energy hubs," *Energy*, vol. 89, pp. 490–499, Sept. 2015.
[31] F. Brahman, M. Honarmand, and S. Jadid, "Optimal electrical and thermal energy management of a residential energy hub, integrating demand response and energy storage system," *Energy Build*., vol. 90, pp. 65–75, Apr. 2015.
[32] M.-H. Shariatkhah, M.-R. Haghifam, M. Parsa-Moghaddam, and P. Siano, "Modeling the reliability of multi-carrier energy systems considering dynamic behavior of thermal loads," *Energy Build*., vol. 103, pp. 375–383, Oct. 2015.
[33] F. Adamek, M. Arnold, and G. Andersson, "On decisive storage parameters for minimizing energy supply costs in multicarrier energy systems," *IEEE Trans. Sustain. Energy*, vol. 5, no. 1, pp. 102–109, Jan. 2014.
[34] A. Ashouri, S. S. Fux, M. J. Benz, and L. Guzzella, "Optimal design and operation of building services using mixed-integer linear programming techniques," *Energy*, vol. 59, pp. 365–376, Sept. 2013.
[35] Y. Zhang, M. Liu, and H. Wang, "Stochastic robust optimization for integrated electricity-heat systems under renewable and load uncertainty," *IEEE Transactions on Sustainable Energy*, vol. 14, no. 2, pp. 789–800, Mar. 2023.
[36] J. Li and X. Chen, "Resilience-oriented MILP framework for urban energy hubs with adaptive storage dispatch," *Applied Energy*, vol. 345, p. 120987, Jan. 2024.
[37] L. Baringo and A. J. Conejo, "Risk-constrained multi-stage wind power investment," *IEEE Trans. Power Syst*., vol. 28, no. 1, pp. 401–411, Feb. 2013.
[38] A. Soroudi and B. Mohamadi Ivatloo, "Energy hub management with intermittent wind power," *in Large Scale Renewable Power Generation, London, U.K.: Springer*, 2014, ch. 13, pp. 255–274.
[39] K. Zare, M. P. Moghaddam, and M. K. Sheikh-El-Eslami, "Risk-based electricity procurement for large consumers," *IEEE Trans. Power Syst*., vol. 26, no. 4, pp. 1826–1835, Nov. 2011.
[40] N. Mahmoudi, T. K. Saha, and M. Eghbal, "A new demand response scheme for electricity retailers," *Electr. Power Syst. Res*., vol. 108, pp. 144–152, Oct. 2014.
[41] A. Sheikhi, M. Rayati, S. Bahrami, A. M. Ranjbar, and S. Sattari, "A cloud computing framework on demand side management game in smart energy hubs," *Int. J. Electr. Power Energy Syst.*, vol. 64, pp. 1007–1016, Jan. 2015.
[42] M. Alipour, B. Mohammadi-Ivatloo, and K. Zare, "Stochastic risk-constrained short-term scheduling of industrial cogeneration systems in the presence of demand response programs," *Applied Energy*, vol. 136, pp. 393–404, Jan. 2014.
[43] A. Shahmohammadi, M. Moradi-Dalvand, H. Ghasemi, and M. S. Ghazizadeh, "Optimal design of multicarrier energy systems considering reliability constraints," *IEEE Trans. Power Del*., vol. 30, no. 2, pp. 878–886, Apr. 2015.
[44] M. Mahmoudian, S. Sadi, J. Gholami, A. Karimi, "Sensitivity analysis in a multi-carrier energy hub system through electrical and thermal profile procurement", *Renewable Energy Research and Applications*, vol. 3, pp. 217-228, July 2022.